

Refractive Index of Humid Air in the Infrared: Model Fits

Richard J. Mathar*

Leiden Observatory, Leiden University, P.O. Box 9513, 2300 RA Leiden, The Netherlands

(Dated: February 2, 2008)

The theory of summation of electromagnetic line transitions is used to tabulate the Taylor expansion of the refractive index of humid air over the basic independent parameters (temperature, pressure, humidity, wavelength) in five separate infrared regions from the H to the Q band at a fixed percentage of Carbon Dioxide. These are least-squares fits to raw, highly resolved spectra for a set of temperatures from 10 to 25 °C, a set of pressures from 500 to 1023 hPa, and a set of relative humidities from 5 to 60%. These choices reflect the prospective application to characterize ambient air at mountain altitudes of astronomical telescopes.

PACS numbers: 51.70.+f, 42.68.-w, 95.85H_p, 92.60.Ta, 41.20.-q

Keywords: refractive index; infrared; water vapor; humid air; phase velocity

I. SCOPE

The paper provides easy access to predictions of the refractive index of humid air at conditions that are typical in atmospheric physics, in support of ray tracing [5] and astronomical applications [4, 16, 47, 50] until experimental coverage of the infrared wavelengths might render these obsolete. The approach is in continuation of earlier work [46] based on a more recent HITRAN database [60] plus more precise accounting of various electromagnetic effects for the dielectric response of dilute gases, as described below.

The literature of optical, chemical and atmospheric physics on the subject of the refractive index of moist air falls into several categories, sorted with respect to decreasing relevance (if relevance is measured by the closeness to experimental data and the degree of independence to the formalism employed here):

1. experiments on moist air in the visible [3, 9, 18, 53],
2. experiments on pure water vapor at 3.4 and 10.6 μm [44, 48, 49],
3. experiments on dry air and its molecular constituents in the visible [6, 23, 32, 78], at 1.064 μm [56, 72], up to 2.0 μm [57], up to 1.7 μm [34, 54, 58, 59], or at 10.6 μm [43, 66],
4. verification of the dispersion and higher order derivatives with astronomical interferometry [71],
5. review formulas [14, 35, 55, 63],
6. theoretical summation of electronic transitions [16, 30, 31, 46].

The liquid and solid states of water are left aside, because extrapolation of their dielectric response to the

gaseous state is difficult by the permanent dipole moment of the molecule. Already in the Q band and then at sub-millimeter wavelengths [42, 61, 79] and eventually in the static limit [24], the refractive index plotted as a function of wavelength is more and more structured by individual lines. Since we will not present these functions at high resolution but smooth fits within several bands in the infrared, their spiky appearance sets a natural limit to the far-IR wavelength regions that our approach may cover.

II. DIELECTRIC MODEL

A. Methodology

The complex valued dielectric function $n(\omega)$ of air

$$n = \sqrt{1 + \bar{\chi}} \quad (1)$$

is constructed from molecular dynamical polarizabilities

$$\chi_m(\omega) = 2N_m c^2 \sum_l \frac{S_{ml}}{\omega_{0ml}} \left(\frac{1}{\omega + \omega_{0ml} - i\Gamma_{ml}/2} - \frac{1}{\omega - \omega_{0ml} - i\Gamma_{ml}/2} \right). \quad (2)$$

N_m are molecular number densities, S_{ml} are the line intensities for the transitions enumerated by l . ω_{0ml} are the transition angular frequencies, Γ_{ml} the full linewidths at half maximum. c is the velocity of light in vacuum, and i the imaginary unit. The line shape (2) adheres to the complex-conjugate symmetry $\chi_m(\omega) = \chi_m^*(-\omega)$, as required for functions which are real-valued in the time domain. The sign convention of Γ_{ml} merely reflects a sign choice in the Fourier Transforms and carries no real significance; a sign in the Kramers–Kronig formulas is bound to it. The integrated imaginary part is [28]

$$\int_0^\infty \Im \chi_m(\tilde{\nu}) d\tilde{\nu} = N_m \sum_l \frac{S_{ml}}{k_{0ml}}, \quad (3)$$

where $\tilde{\nu} = k/(2\pi) = \omega/(2\pi c) = 1/\lambda$ is the wavenumber.

*Electronic address: mathar@strw.leidenuniv.nl;
URL: <http://www.strw.leidenuniv.nl/~mathar>

Line strengths S_{ml} and positions ω_{0ml} are based on the HITRAN [60] list (see [68, 69] for reviews) and other sources as described earlier [46]. The results of Section IV include summation over the oscillator strengths of the air components N₂, O₂, Ar, Ne, CO₂, H₂O, O₃, CH₄ and CO. Fig. 1 is an estimate of the combined contribution of tracer gases that are missing in this mix of molecules—and effectively replaced by the average refractivity of the major components—sorted with respect to abundance under rather clean environmental conditions. Their electromagnetic line lists are taken from [41, 75] for He, [11] for Kr, [45] for H₂, [45, 60] for N₂O, [60] for SO₂, and [45, 60] for NH₃.

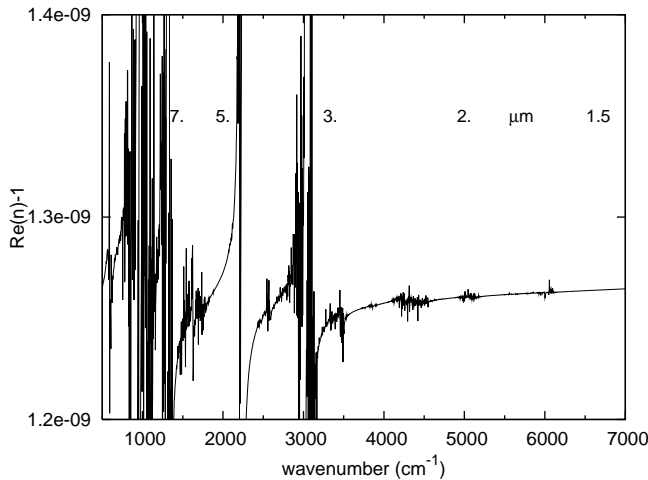


FIG. 1: The combined refractivity of 0.39 Pa He, 0.075 Pa Kr, 0.038 Pa H₂, 0.030 Pa NH₃, 0.023 Pa N₂O, and 3.8×10^{-5} Pa SO₂, is $\approx 10^{-9}$ at 12 °C. The dispersion (change in the refractivity) across the relevant bands in the IR is $\approx 10^{-10}$.

The remaining subsections describe some refinements of the computer program relative to its status three years ago [46].

B. Deviations from Ideal Gas Behavior

The second virial coefficients for Nitrogen and Oxygen are negative at typical environmental temperatures, $\approx -7.5 \times 10^{-6}$ m³/mole for Nitrogen and $\approx -1.9 \times 10^{-5}$ m³/mole for Oxygen at 12 °C [22, 74]. More molecules are packed into a given volume at a given partial pressure than the ideal gas equation predicts. The gas densities of Nitrogen and Oxygen are ≈ 25 mole/m³ and ≈ 6 mole/m³ for Nitrogen and Oxygen, respectively, at air pressures of the order 740 hPa, so the correction factors for the density and for the refractivity are of the order 2×10^{-4} due to this effect, the product of the virial and the density. See [40] for a review and [1] for examples of the crosstalk to refractivities.

The second and third virials for water vapor are larger [29, 37, 39]—the second $\approx -1.3 \times 10^{-3}$ m³/mole [73, Fig

7.19]—and often placed as “enhancement factors.” See [62] for a review on this subject and [26] for recent values of the second virial coefficient. The values presented here use the equation of state in a self-consistent solution of the first line of [73, Tab. 6.3] for water, the values of [22, p. 239] for Nitrogen, and the NIST values [52] for the second and third virials of Oxygen, Argon and Carbon Dioxide.

C. Temperature Dependent Partition Sums

The temperature dependence of the partition sums leads to temperature-dependent line strengths [2]. For the HITRAN lines, this has been implemented on a line-per-line basis [25, 65]. The combined change induced by the upgrade to the database of August '06 plus this increase of the line strengths at lower temperatures is minuscule, less than 2×10^{-9} in the $c_{0\text{ref}}$ coefficients and less than 3×10^{-5} K in the c_{0T} coefficients reported in Section IV.

The line broadening parameters Γ were not changed [33, 70] from the ones at the HITRAN reference pressure of 1 atm, since the effect on the real part of the susceptibility is presumably negligible. Effects of molecular clustering [67] have not been considered.

D. Magnetic Susceptibility

The paramagnetic susceptibility of Oxygen and diamagnetic contribution of Nitrogen [27] account for most of the remaining gap between theory and experiment. The volume susceptibility of dry air is $\approx 3.7 \times 10^{-7}$ [19] at 1013 hPa, to increase n by $\approx 1.3 \times 10^{-7}$. The magnetic dipole transitions of Oxygen [10, 38] are incorporated in the HITRAN list [13], which allows us to add dispersion to their response. (Since we are only dealing with the limit of small susceptibilities, the electric and magnetic susceptibilities are additive, which means cross product terms have been neglected here.) The magnetism of water is negligible because the magnetic moment of the water molecule is close to the magnetic moment of the Nitrogen molecule [15, 19], but the abundance of the water molecules in air much smaller than the abundance of Nitrogen molecules.

E. Lorentz-Lorenz Cross Polarization

We incorporate the mutual inter-molecular cross-polarization with the Clausius-Mossotti (Lorentz-Lorenz) formula [20, 21]: the macroscopic susceptibility $\bar{\chi} = n^2 - 1$ in Eq. (1). is

$$\bar{\chi} = \frac{\sum \chi_m}{1 - \sum \chi_m/3}, \quad (4)$$

where $\sum \chi_m$ is the sum over all atomic/molecular polarizabilities. This increases the real part of χ by $\approx (\sum \chi_m)^2/3$, hence the real part of n by $\approx (\sum \chi_m)^2/6$, which is of the order 2×10^{-8} if we take $\sum_m \chi \approx 4 \times 10^{-4}$ as a guideline.

III. COMPARISON WITH EXPERIMENTS

The raw theoretical data (prior to the fit) exceeds experiments for dry air in the visible and near infrared by $\approx 4 \times 10^{-8}$ (Fig. 2). Roughly 0.8×10^{-8} of this can be attributed to a change in temperature scales [7], and roughly 1×10^{-8} to a presumably lower CO₂ contents of 300 ppmv in [58].

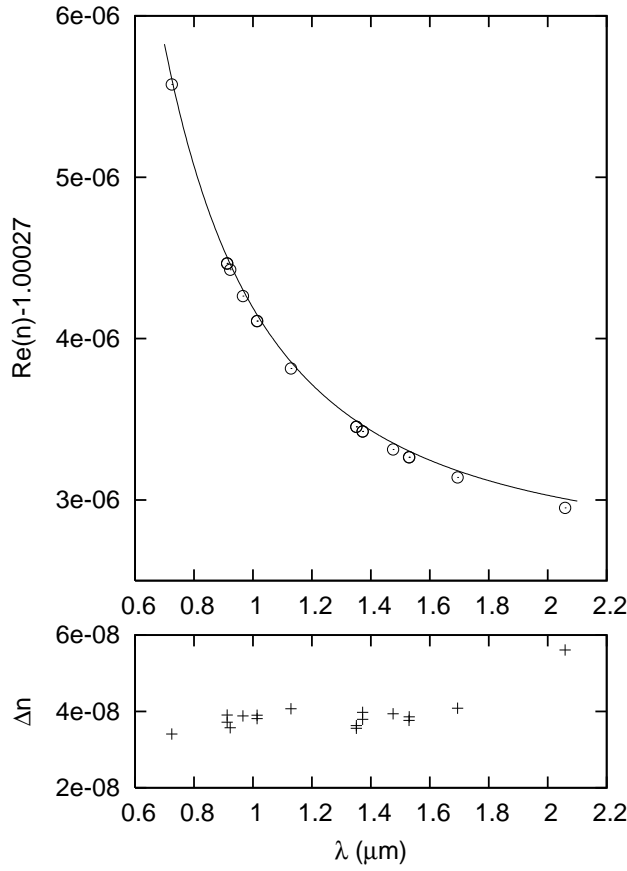


FIG. 2: Top: The line are the raw data of the theory for dry air at 15 °C and 101324 Pa. Circles are the experimental values of Table I and II by Peck and Reeder [58] plus one datum at 2.06 μm by Peck and Khanna [57]. Bottom: Refractive index of the theory minus these experimental values.

The pressure coefficient c_{0p} for dry air at 10 μm in Table IV is to be compared to the value of $2.668 \times 10^{-4}/\text{atm} = 0.2633 \times 10^{-8}/\text{Pa}$ measured at $\lambda = 10.57 \mu\text{m}$ and $T = 23$ °C by Marchetti and Simili [43, Tab. 1]. More accurately, the pressure gradient predicted from (7)

is

$$\frac{\partial n}{\partial p} = \sum_{i=0,1,\dots} \left[c_{ip} + 2c_{ipp} (p - p_{\text{ref}}) + c_{iT} \left(\frac{1}{T} - \frac{1}{T_{\text{ref}}} \right) + c_{iH} (H - H_{\text{ref}}) \right] (\tilde{\nu} - \tilde{\nu}_{\text{ref}})^i \quad (5)$$

and generates $0.2618 \times 10^{-8}/\text{Pa}$ at the same wavelength, the same temperature, and a pressure—undocumented by Marchetti and Simili—of 1013.25 hPa. The relative deviation of 6×10^{-3} between experiment and theory is still compatible with the error 5×10^{-3} provided by Marchetti and Simili.

The theory deviates from the humid air data at the longest two wavelengths of the Bönsch-Potulski experiments [9] by 3.5×10^{-8} or less: Fig. 3.

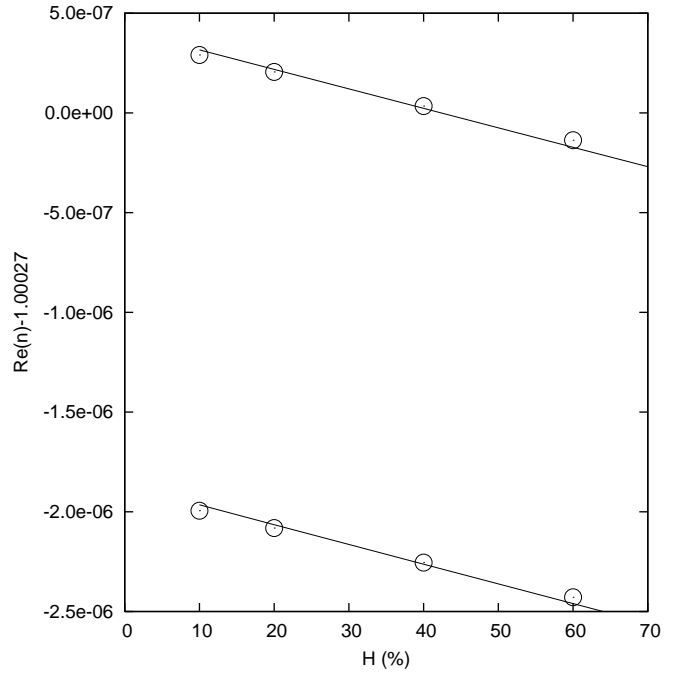


FIG. 3: Lines are the raw data of the theory for humid air at 20 °C and 1000 hPa at four levels of humidity. Circles are from the Bönsch-Potulski fitting equation (at 370 ppm CO₂) to their experimental data [9]. The two groups of four comparisons refer to the wavelengths 0.5087 and 0.644 μm .

The difference between the theory and experiments with pure water vapor (Fig. 4) and moist air (Fig. 5) is $\approx 1 \times 10^{-8}$ at 3.4 μm .

IV. RESULTS

The bold least squares fit to the raw data—examples of which are shown in [47, Figs. 2,12]—looks as follows:

$$n - 1 = \sum_{i=0,1,2,\dots} c_i(T, p, H) (\tilde{\nu} - \tilde{\nu}_{\text{ref}})^i; \quad (6)$$

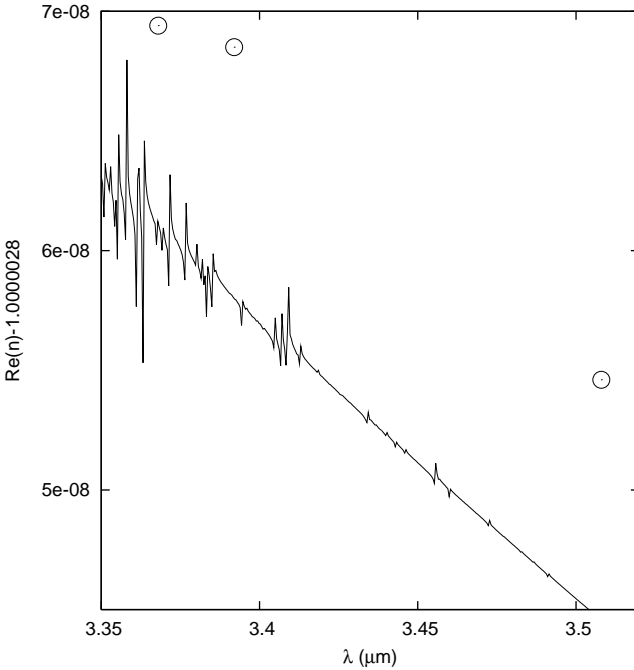


FIG. 4: Comparison of the theory (solid line) with the experimental data by Matsumoto (3 circles) [48, Tab. 1] for water vapor of 1333 Pa at 20 °C.

$$\begin{aligned}
c_i(T, p, H) = & c_{i\text{ref}} \\
& + c_{iT} \left(\frac{1}{T} - \frac{1}{T_{\text{ref}}} \right) + c_{iTT} \left(\frac{1}{T} - \frac{1}{T_{\text{ref}}} \right)^2 \\
& + c_{iH} (H - H_{\text{ref}}) + c_{iHH} (H - H_{\text{ref}})^2 \\
& + c_{ip} (p - p_{\text{ref}}) + c_{ipp} (p - p_{\text{ref}})^2 \\
& + c_{iTH} \left(\frac{1}{T} - \frac{1}{T_{\text{ref}}} \right) (H - H_{\text{ref}}) \\
& + c_{iTp} \left(\frac{1}{T} - \frac{1}{T_{\text{ref}}} \right) (p - p_{\text{ref}}) \\
& + c_{iHP} (H - H_{\text{ref}}) (p - p_{\text{ref}}). \quad (7)
\end{aligned}$$

Here, T is the absolute temperature with a reference value of $T_{\text{ref}} = (273.15 + 17.5)$ K, p is the air pressure with a reference value set at $p_{\text{ref}} = 75000$ Pa, H the relative humidity between 0 and 100 with a reference value set at $H_{\text{ref}} = 10$ %, and $\tilde{\nu}$ the wavenumber $1/\lambda$ with a reference value set at $\tilde{\nu}_{\text{ref}}$. The units of these reference values match those of the tabulated coefficients. The range 1.3–2.5 μm is covered by Table I, the range 2.8–4.2 μm by Table II, the range 4.35–5.3 μm by Table III, the range 7.5–14.1 μm by Table IV, and the range 16–20 μm by Table V. The refractive index is chromatic (the phase shift depends on the wavelength λ and wave number $\tilde{\nu}$) since

$$dn/d\lambda = -\tilde{\nu}^2 \frac{dn}{d\tilde{\nu}} \quad (8)$$

depends itself on λ . (The negative of this parameter, measured in radian and divided by the areal molar gas

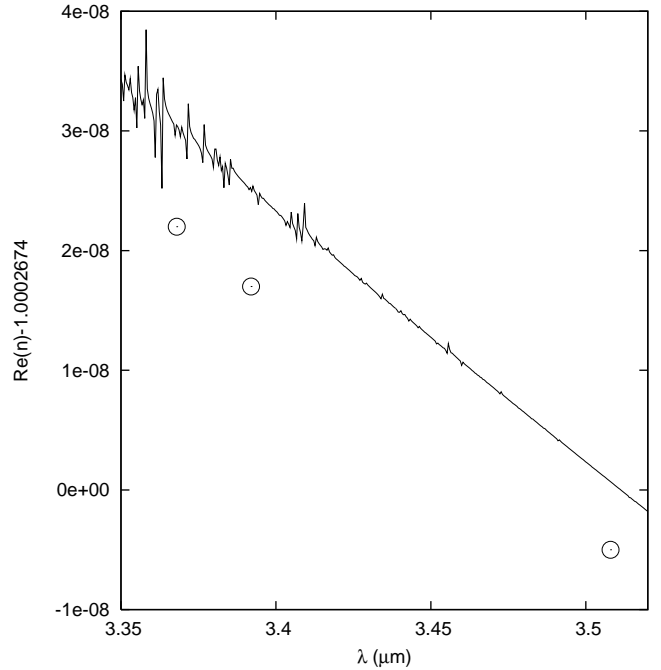


FIG. 5: Comparison of the theory (solid line, 300 ppmv CO₂) with the experimental data by Matsumoto (3 circles) [48, Tab. 2] for humid air at $p = 1013.25$ hPa, $T = 20$ °C and $H = 56.98$ %.

density, has been baptized “normalized dispersion constant” K in [50, 51].) Our simple analytical fit format allows rapid calculation of group refractive indices as well [47].

The calculation adopts a standard of 370 ppmv of CO₂ as the most likely contemporary ambient clean air standard [17, 36, 77], well aware that laboratory air may contain a higher volume fraction. Although adding this mixing ratio as another free parameter to the procedure is feasible, it has been kept fixed here to keep the size of the tables in check.

The use of $1/T$ rather than T in the ansatz (7) has no further relevance but aims to expand the validity of the results to a large range of temperatures: in the simplest model of the dispersion one expects the susceptibility to be proportional to the molecular densities which are—with the ideal gas equation—proportional to p/T . This reasoning is actually void—as demonstrated by the magnitudes of c_{iTT} —because we are employing non-infinite reference temperatures T_{ref} .

Solely for the benefit of the reader who may use this type of result as a black box, the parameter set in (7) is based on relative humidity rather than some more fundamental measure of the water molecule number density; the more appealing alternative from a scholarly point of view would have been to split the computational steps into (i) equations to calculate absolute molecular number densities, plus (ii) the fitting equations to transform these to polarizabilities, and (iii) some post-processing

TABLE I: Fitting coefficients for the multivariate Taylor expansion (7) to the real part of the index of refraction over the $1.3 \leq 1/\tilde{\nu} \leq 2.5 \mu\text{m}$ range with $\tilde{\nu}_{\text{ref}} = 10^4/2.25 \text{ cm}^{-1}$.

i	$c_{i\text{ref}} / \text{cm}^i$	$c_{iT} / \text{cm}^i \text{K}$	$c_{iTT} / [\text{cm}^i \text{K}^2]$	$c_{iH} / [\text{cm}^i / \%]$	$c_{iHH} / [\text{cm}^i / \%^2]$
0	0.200192×10^{-3}	0.588625×10^{-1}	-3.01513	-0.103945×10^{-7}	0.573256×10^{-12}
1	0.113474×10^{-9}	-0.385766×10^{-7}	0.406167×10^{-3}	0.136858×10^{-11}	0.186367×10^{-16}
2	$-0.424595 \times 10^{-14}$	0.888019×10^{-10}	-0.514544×10^{-6}	$-0.171039 \times 10^{-14}$	$-0.228150 \times 10^{-19}$
3	0.100957×10^{-16}	$-0.567650 \times 10^{-13}$	0.343161×10^{-9}	0.112908×10^{-17}	0.150947×10^{-22}
4	$-0.293315 \times 10^{-20}$	0.166615×10^{-16}	$-0.101189 \times 10^{-12}$	$-0.329925 \times 10^{-21}$	$-0.441214 \times 10^{-26}$
5	0.307228×10^{-24}	$-0.174845 \times 10^{-20}$	0.106749×10^{-16}	0.344747×10^{-25}	0.461209×10^{-30}

i	$c_{ip} / [\text{cm}^i / \text{Pa}]$	$c_{ipp} / [\text{cm}^i / \text{Pa}^2]$	$c_{iTH} / [\text{cm}^i \text{K} / \%]$	$c_{iT_P} / [\text{cm}^i \text{K} / \text{Pa}]$	$c_{iH_P} / [\text{cm}^i / (\% \text{ Pa})]$
0	0.267085×10^{-8}	0.609186×10^{-17}	0.497859×10^{-4}	0.779176×10^{-6}	$-0.206567 \times 10^{-15}$
1	0.135941×10^{-14}	0.519024×10^{-23}	-0.661752×10^{-8}	0.396499×10^{-12}	0.106141×10^{-20}
2	0.135295×10^{-18}	$-0.419477 \times 10^{-27}$	0.832034×10^{-11}	0.395114×10^{-16}	$-0.149982 \times 10^{-23}$
3	0.818218×10^{-23}	0.434120×10^{-30}	$-0.551793 \times 10^{-14}$	0.233587×10^{-20}	0.984046×10^{-27}
4	$-0.222957 \times 10^{-26}$	$-0.122445 \times 10^{-33}$	0.161899×10^{-17}	$-0.636441 \times 10^{-24}$	$-0.288266 \times 10^{-30}$
5	0.249964×10^{-30}	0.134816×10^{-37}	$-0.169901 \times 10^{-21}$	0.716868×10^{-28}	0.299105×10^{-34}

TABLE II: Fitting coefficients for the multivariate Taylor expansion (7) to the real part of the index of refraction over the $2.8 \leq 1/\tilde{\nu} \leq 4.2 \mu\text{m}$ range with $\tilde{\nu}_{\text{ref}} = 10^4/3.4 \text{ cm}^{-1}$.

i	$c_{i\text{ref}} / \text{cm}^i$	$c_{iT} / \text{cm}^i \text{K}$	$c_{iTT} / [\text{cm}^i \text{K}^2]$	$c_{iH} / [\text{cm}^i / \%]$	$c_{iHH} / [\text{cm}^i / \%^2]$
0	0.200049×10^{-3}	0.588431×10^{-1}	-3.13579	-0.108142×10^{-7}	0.586812×10^{-12}
1	0.145221×10^{-9}	-0.825182×10^{-7}	0.694124×10^{-3}	0.230102×10^{-11}	0.312198×10^{-16}
2	0.250951×10^{-12}	0.137982×10^{-9}	-0.500604×10^{-6}	$-0.154652 \times 10^{-14}$	$-0.197792 \times 10^{-19}$
3	$-0.745834 \times 10^{-15}$	0.352420×10^{-13}	-0.116668×10^{-8}	$-0.323014 \times 10^{-17}$	$-0.461945 \times 10^{-22}$
4	$-0.161432 \times 10^{-17}$	$-0.730651 \times 10^{-15}$	0.209644×10^{-11}	0.630616×10^{-20}	0.788398×10^{-25}
5	0.352780×10^{-20}	$-0.167911 \times 10^{-18}$	0.591037×10^{-14}	0.173880×10^{-22}	0.245580×10^{-27}

i	$c_{ip} / [\text{cm}^i / \text{Pa}]$	$c_{ipp} / [\text{cm}^i / \text{Pa}^2]$	$c_{iTH} / [\text{cm}^i \text{K} / \%]$	$c_{iT_P} / [\text{cm}^i \text{K} / \text{Pa}]$	$c_{iH_P} / [\text{cm}^i / (\% \text{ Pa})]$
0	0.266900×10^{-8}	0.608860×10^{-17}	0.517962×10^{-4}	0.778638×10^{-6}	$-0.217243 \times 10^{-15}$
1	0.168162×10^{-14}	0.461560×10^{-22}	-0.112149×10^{-7}	0.446396×10^{-12}	0.104747×10^{-20}
2	0.353075×10^{-17}	0.184282×10^{-24}	0.776507×10^{-11}	0.784600×10^{-15}	$-0.523689 \times 10^{-23}$
3	$-0.963455 \times 10^{-20}$	$-0.524471 \times 10^{-27}$	0.172569×10^{-13}	$-0.195151 \times 10^{-17}$	0.817386×10^{-26}
4	$-0.223079 \times 10^{-22}$	$-0.121299 \times 10^{-29}$	$-0.320582 \times 10^{-16}$	$-0.542083 \times 10^{-20}$	0.309913×10^{-28}
5	0.453166×10^{-25}	0.246512×10^{-32}	$-0.899435 \times 10^{-19}$	0.103530×10^{-22}	$-0.363491 \times 10^{-31}$

with (4). The first step involves a self-consistent adaptation of the components of the dry air at given mixing ratios to a partial pressure that is “left over” from p after settling for the water density. The philosophy behind Equation (7) is to take this kind of burden away.

The negative values of c_{0H} paraphrase that substitution of the “average” dry air molecule by water at fixed total pressures p decreases the refractive index in all our wavelength regions.

Acknowledgments

This work is supported by the NWO VICI grant of 15-6-2003 “Optical Interferometry: A new Method for Studies of Extrasolar Planets” to A. Quirrenbach.

[1] Achtermann, H. J., G. Magnus, and T. K. Bose, 1991, *J. Chem. Phys.* **94**(8), 5669.

[2] Barber, R. J., J. Tennyson, G. J. Harris, and R. N. Tolchenov, 2006, *Month. Not. Roy. Astron. Soc.* **368**(3),

TABLE III: Fitting coefficients for the multivariate Taylor expansion (7) to the real part of the index of refraction over the $4.35 \leq 1/\tilde{\nu} \leq 5.3 \mu\text{m}$ range with $\tilde{\nu}_{\text{ref}} = 10^4/4.8 \text{ cm}^{-1}$.

i	$c_{i\text{ref}} / \text{cm}^i$	$c_{iT} / \text{cm}^i \text{K}$	$c_{iTT} / [\text{cm}^i \text{K}^2]$	$c_{iH} / [\text{cm}^i / \%]$	$c_{iHH} / [\text{cm}^i / \%^2]$
0	0.200020×10^{-3}	0.590035×10^{-1}	-4.09830	-0.140463×10^{-7}	0.543605×10^{-12}
1	0.275346×10^{-9}	-0.375764×10^{-6}	0.250037×10^{-2}	0.839350×10^{-11}	0.112802×10^{-15}
2	0.325702×10^{-12}	0.134585×10^{-9}	0.275187×10^{-6}	$-0.190929 \times 10^{-14}$	$-0.229979 \times 10^{-19}$
3	$-0.693603 \times 10^{-14}$	0.124316×10^{-11}	-0.653398×10^{-8}	$-0.121399 \times 10^{-16}$	$-0.191450 \times 10^{-21}$
4	0.285610×10^{-17}	0.508510×10^{-13}	-0.310589×10^{-9}	$-0.898863 \times 10^{-18}$	$-0.120352 \times 10^{-22}$
5	0.338758×10^{-18}	$-0.189245 \times 10^{-15}$	0.127747×10^{-11}	0.364662×10^{-20}	0.500955×10^{-25}

i	$c_{ip} / [\text{cm}^i / \text{Pa}]$	$c_{ipp} / [\text{cm}^i / \text{Pa}^2]$	$c_{iTH} / [\text{cm}^i \text{K} / \%]$	$c_{iT_p} / [\text{cm}^i \text{K} / \text{Pa}]$	$c_{iH_p} / [\text{cm}^i / (\% \text{ Pa})]$
0	0.266898×10^{-8}	0.610706×10^{-17}	0.674488×10^{-4}	0.778627×10^{-6}	$-0.211676 \times 10^{-15}$
1	0.273629×10^{-14}	0.116620×10^{-21}	-0.406775×10^{-7}	0.593296×10^{-12}	0.487921×10^{-20}
2	0.463466×10^{-17}	0.244736×10^{-24}	0.289063×10^{-11}	0.145042×10^{-14}	$-0.682545 \times 10^{-23}$
3	$-0.916894 \times 10^{-19}$	$-0.497682 \times 10^{-26}$	0.819898×10^{-13}	0.489815×10^{-17}	0.942802×10^{-25}
4	0.136685×10^{-21}	0.742024×10^{-29}	0.468386×10^{-14}	0.327941×10^{-19}	$-0.946422 \times 10^{-27}$
5	0.413687×10^{-23}	0.224625×10^{-30}	$-0.191182 \times 10^{-16}$	0.128020×10^{-21}	$-0.153682 \times 10^{-29}$

TABLE IV: Fitting coefficients for the multivariate Taylor expansion (7) to the real part of the index of refraction over the $7.5 \leq 1/\tilde{\nu} \leq 14.1 \mu\text{m}$ range with $\tilde{\nu}_{\text{ref}} = 10^4/10.1 \text{ cm}^{-1}$.

i	$c_{i\text{ref}} / \text{cm}^i$	$c_{iT} / \text{cm}^i \text{K}$	$c_{iTT} / [\text{cm}^i \text{K}^2]$	$c_{iH} / [\text{cm}^i / \%]$	$c_{iHH} / [\text{cm}^i / \%^2]$
0	0.199885×10^{-3}	0.593900×10^{-1}	-6.50355	-0.221938×10^{-7}	0.393524×10^{-12}
1	0.344739×10^{-9}	-0.172226×10^{-5}	0.103830×10^{-1}	0.347377×10^{-10}	0.464083×10^{-15}
2	$-0.273714 \times 10^{-12}$	0.237654×10^{-8}	-0.139464×10^{-4}	$-0.465991 \times 10^{-13}$	$-0.621764 \times 10^{-18}$
3	0.393383×10^{-15}	$-0.381812 \times 10^{-11}$	0.220077×10^{-7}	0.735848×10^{-16}	0.981126×10^{-21}
4	$-0.569488 \times 10^{-17}$	0.305050×10^{-14}	$-0.272412 \times 10^{-10}$	$-0.897119 \times 10^{-19}$	$-0.121384 \times 10^{-23}$
5	0.164556×10^{-19}	$-0.157464 \times 10^{-16}$	0.126364×10^{-12}	0.380817×10^{-21}	0.515111×10^{-26}

i	$c_{ip} / [\text{cm}^i / \text{Pa}]$	$c_{ipp} / [\text{cm}^i / \text{Pa}^2]$	$c_{iTH} / [\text{cm}^i \text{K} / \%]$	$c_{iT_p} / [\text{cm}^i \text{K} / \text{Pa}]$	$c_{iH_p} / [\text{cm}^i / (\% \text{ Pa})]$
0	0.266809×10^{-8}	0.610508×10^{-17}	0.106776×10^{-3}	0.778368×10^{-6}	$-0.206365 \times 10^{-15}$
1	0.695247×10^{-15}	0.227694×10^{-22}	-0.168516×10^{-6}	0.216404×10^{-12}	0.300234×10^{-19}
2	0.159070×10^{-17}	0.786323×10^{-25}	0.226201×10^{-9}	0.581805×10^{-15}	$-0.426519 \times 10^{-22}$
3	$-0.303451 \times 10^{-20}$	$-0.174448 \times 10^{-27}$	$-0.356457 \times 10^{-12}$	$-0.189618 \times 10^{-17}$	0.684306×10^{-25}
4	$-0.661489 \times 10^{-22}$	$-0.359791 \times 10^{-29}$	0.437980×10^{-15}	$-0.198869 \times 10^{-19}$	$-0.467320 \times 10^{-29}$
5	0.178226×10^{-24}	0.978307×10^{-32}	$-0.194545 \times 10^{-17}$	0.589381×10^{-22}	0.126117×10^{-30}

1087.

[3] Barrell, H., and J. E. Sears, 1939, *Phil. Trans. R. Soc. A* **238**(786), 1.

[4] Basden, A. G., and D. F. Buscher, 2005, *Month. Not. Roy. Astron. Soc.* **357**(2), 656.

[5] Berton, R. P. H., 2006, *J. Opt. A: Pure Appl. Opt.* **8**(10), 817.

[6] Birch, K. P., 1991, *J. Opt. Soc. Am. A* **8**(4), 647.

[7] Birch, K. P., and M. J. Downs, 1993, *Metrologia* **30**, 155, E: [8].

[8] Birch, K. P., and M. J. Downs, 1994, *Metrologia* **31**(4), 315.

[9] Bönsch, G., and E. Potulski, 1998, *Metrologia* **35**, 133.

[10] Boreiko, R. T., T. L. Smithson, T. A. Clark, and H. Wieser, 1984, *J. Quant. Spectrosc. Radiat. Transfer* **32**(2), 109.

[11] Chan, W. F., G. Cooper, X. Guo, G. R. Burton, and C. E. Brion, 1992, *Phys. Rev. A* **46**(1), 149, E: [12].

[12] Chan, W. F., G. Cooper, X. Guo, G. R. Burton, and C. E. Brion, 1993, *Phys. Rev. A* **48**(1), 858.

[13] Chance, K. V., W. A. Traub, K. W. Jucks, and D. G. Johnson, 1991, *Int. J. Infrared Millimeter Waves* **12**(6), 581.

[14] Ciddor, P. E., 1996, *Appl. Opt.* **35**(9), 1566.

[15] Cini, R., and M. Torrini, 1968, *J. Chem. Phys.* **49**(6), 2826.

[16] Colavita, M. M., M. R. Swain, R. L. Akeson, C. D. Koresko, and R. J. Hill, 2004, *Publ. Astron. Soc. Pac.* **116**(823), 876.

[17] Cooperative Atmospheric Data Integration Project, 2003, *GLOBALVIEW-CO₂*, Technical Report, NOAA/CMDL, URL

TABLE V: Fitting coefficients for the multivariate Taylor expansion (7) to the real part of the index of refraction over the $16 \leq 1/\tilde{\nu} \leq 28 \mu\text{m}$ range with $\tilde{\nu}_{\text{ref}} = 10^4/20 \text{ cm}^{-1}$.

i	$c_{i\text{ref}} / \text{cm}^i$	$c_{iT} / \text{cm}^i \text{K}$	$c_{iT\text{T}} / [\text{cm}^i \text{K}^2]$	$c_{iH} / [\text{cm}^i / \%]$	$c_{iHH} / [\text{cm}^i / \%^2]$
0	0.199436×10^{-3}	0.621723×10^{-1}	-23.2409	-0.772707×10^{-7}	$-0.326604 \times 10^{-12}$
1	0.299123×10^{-8}	-0.177074×10^{-4}	0.108557	0.347237×10^{-9}	0.463606×10^{-14}
2	$-0.214862 \times 10^{-10}$	0.152213×10^{-6}	-0.102439×10^{-2}	$-0.272675 \times 10^{-11}$	$-0.364272 \times 10^{-16}$
3	0.143338×10^{-12}	-0.954584×10^{-9}	0.634072×10^{-5}	0.170858×10^{-13}	0.228756×10^{-18}
4	0.122398×10^{-14}	$-0.996706 \times 10^{-11}$	0.762517×10^{-7}	0.156889×10^{-15}	0.209502×10^{-20}
5	$-0.114628 \times 10^{-16}$	0.921476×10^{-13}	-0.675587×10^{-9}	$-0.150004 \times 10^{-17}$	$-0.200547 \times 10^{-22}$

i	$c_{ip} / [\text{cm}^i / \text{Pa}]$	$c_{ipp} / [\text{cm}^i / \text{Pa}^2]$	$c_{iTH} / [\text{cm}^i \text{K} / \%]$	$c_{iT\text{p}} / [\text{cm}^i \text{K} / \text{Pa}]$	$c_{iH\text{p}} / [\text{cm}^i / (\% \text{ Pa})]$
0	0.266827×10^{-8}	0.613675×10^{-17}	0.375974×10^{-3}	0.778436×10^{-6}	$-0.272614 \times 10^{-15}$
1	0.120788×10^{-14}	0.585494×10^{-22}	-0.171849×10^{-5}	0.461840×10^{-12}	0.304662×10^{-18}
2	0.522646×10^{-17}	0.286055×10^{-24}	0.146704×10^{-7}	0.306229×10^{-14}	$-0.239590 \times 10^{-20}$
3	0.783027×10^{-19}	0.425193×10^{-26}	$-0.917231 \times 10^{-10}$	$-0.623183 \times 10^{-16}$	0.149285×10^{-22}
4	0.753235×10^{-21}	0.413455×10^{-28}	$-0.955922 \times 10^{-12}$	$-0.161119 \times 10^{-18}$	0.136086×10^{-24}
5	$-0.228819 \times 10^{-24}$	$-0.812941 \times 10^{-32}$	0.880502×10^{-14}	0.800756×10^{-20}	$-0.130999 \times 10^{-26}$

<ftp://ftp.cmdl.noaa.gov/ccg/co2/GLOBALVIEW>.

[18] Cuthbertson, C., and M. Cuthbertson, 1913, Phil. Trans. R. Soc. London A **213**, 1.

[19] Davis, R. S., 1998, Metrologia **35**(4), 49.

[20] de Goede, J., and P. Mazur, 1972, Physica **58**, 568.

[21] de Wolf, D. A., 1993, J. Opt. Soc. Am. A **10**(7), 1544.

[22] Dymond, J. H., and E. B. Smith, 1980, *The virial coefficients of pure gases and mixtures* (Clarendon Press, Oxford).

[23] Edlén, B., 1953, J. Opt. Soc. Am. **43**(5), 339.

[24] Fernández, D. P., Y. Mulev, A. R. H. Goodwin, and J. M. H. Levelt Sengers, 1995, J. Phys. Chem. Ref. Data **24**(1), 33.

[25] Gamache, R. R., S. Kennedy, R. Hawkins, and L. S. Rothman, 2000, J. Mol. Struct. **517–518**, 407.

[26] Harvey, A. H., and E. W. Lemmon, 2004, J. Phys. Chem. Ref. Data **33**(1), 369.

[27] Havens, G. G., 1933, Phys. Rev. **43**(12), 992.

[28] Hilborn, R. C., 1981, Am. J. Phys. **50**(11), 982.

[29] Hill, P. G., and R. D. C. MacMillan, 1988, Ind. Eng. Chem. Res. **27**(5), 874.

[30] Hill, R. J., S. F. Clifford, and R. S. Lawrence, 1980, J. Opt. Soc. Am. **70**(10), 1192.

[31] Hill, R. J., and R. S. Lawrence, 1986, Infrared Phys. **26**(6), 371.

[32] Hou, W., and R. Thalmann, 1994, Measurement **13**, 307.

[33] Jacquemart, D., R. Gamache, and L. S. Rothman, 2005, J. Quant. Spectrosc. Radiat. Transfer **96**, 205.

[34] Jhanwar, B. L., and W. J. Meath, 1982, Chem. Phys. **67**(2), 185.

[35] Jones, F. E., 1980, Appl. Opt. **19**(24), 4129.

[36] Kane, R. P., and E. R. de Paula, 1996, J. Atmosp. Terr. Phys. **58**(15), 1673.

[37] Kell, G. S., G. E. McLaurin, and E. Whalley, 1989, Proc. R. Soc. Lond. A **425**(1868), 49.

[38] Krupenie, P. H., 1972, J. Phys. Chem. Ref. Data **1**(2), 423.

[39] Kusalik, P. G., F. Liden, and I. M. Svishchev, 1995, J. Chem. Phys. **103**(23), 10169.

[40] Lemmon, E. W., R. T. Jacobsen, S. G. Penoncello, and D. G. Friend, 2000, J. Phys. Chem. Ref. Data **29**(3), 331.

[41] Ligtenberg, R. C. G., P. J. M. van der Burgt, S. P. Renwick, W. B. Westerveld, and J. S. Risley, 1994, Phys. Rev. A **49**(4), 2363.

[42] Manabe, T., Y. Furuhama, T. Ihara, S. Saito, H. Tanaka, and A. Ono, 1985, Int. J. Infrared Millimeter Waves **6**(4), 313.

[43] Marchetti, S., and R. Simili, 2006, Infr. Phys. Techn. **47**(3), 263, presumably, the factor 10^{-4} ought read 10^{+4} and the temperature 296 °C read 23 °C in Table 1.

[44] Marchetti, S., and R. Simili, 2006, Infr. Phys. Techn. **48**(2), 115.

[45] Margoliash, D. J., and W. J. Meath, 1978, J. Chem. Phys. **68**(4), 1426.

[46] Mathar, R. J., 2004, Appl. Opt. **43**(4), 928.

[47] Mathar, R. J., 2006, arXiv:astro-ph/0605304 .

[48] Matsumoto, H., 1982, Metrologia **18**(2), 49, we assume that the f -value in Table 2 is 1333, not 133 Pa, and that the three values refer to three different wavelengths—those in Table 1—not two.

[49] Matsumoto, H., 1984, Opt. Commun. **50**(6), 356.

[50] Meisner, J. A., and R. S. Le Poole, 2003, in *Interferometry for Optical Astronomy II*, edited by W. A. Traub (Int. Soc. Optical Engineering), volume 4838 of *Proc. SPIE*, pp. 609–624.

[51] Meisner, J. A., R. N. Tubbs, and W. J. Jaffe, 2004, in *New Frontiers in Stellar Interferometry*, edited by W. A. Traub (Int. Soc. Optical Engineering), volume 5491 of *Proc. SPIE*, pp. 725–740.

[52] Natl. Inst. Stand. Technol., 2006, *Database of the Thermodynamical Properties of Gases Used in Semiconductor Industry*, Technical Report 134, NIST.

[53] Newbound, K. B., 1949, J. Opt. Soc. Am. **39**(10), 835.

[54] Old, J. G., K. L. Gentili, and E. R. Peck, 1971, J. Opt. Soc. Am. **61**(1), 89.

[55] Owens, J. C., 1967, Appl. Opt. **6**(1), 51.

[56] Peck, E. R., 1986, Appl. Opt. **25**(20), 3597.

[57] Peck, E. R., and B. N. Khanna, 1962, J. Opt. Soc. Am.

52(4), 416.

[58] Peck, E. R., and K. Reeder, 1972, *J. Opt. Soc. Am.* **62**(8), 958.

[59] Rank, D. H., G. D. Saksena, and T. K. McCubbin, Jr., 1958, *J. Opt. Soc. Am.* **48**(7), 455.

[60] Rothman, L. S., D. Jacquemart, A. Barbe, D. C. Benner, M. Birk, L. R. Brown, M. R. Carleer, C. Chackerian Jr., K. Chance, L. H. Coudert, V. Dana, V. M. Devi, *et al.*, 2005, *J. Quant. Spectrosc. Radiat. Transfer* **96**, 139.

[61] Rüeger, J. M., 2002, in *Proc. FIG XXII Intl. Congress* (Washington).

[62] Sato, H., K. Watanabe, J. M. H. Levelt Sengers, J. S. Gallagher, P. G. Hill, J. Straub, and W. Wagner, 1991, *J. Phys. Chem. Ref. Data* **20**(5), 1023.

[63] Schiebener, P., J. Straub, J. M. H. Levelt Sengers, and J. S. Gallagher, 1990, *J. Phys. Chem. Ref. Data* **19**(3), 677, E: [64].

[64] Schiebener, P., J. Straub, J. M. H. Levelt Sengers, and J. S. Gallagher, 1990, *J. Phys. Chem. Ref. Data* **19**, 1617.

[65] Simečková, M., D. Jacquemart, L. S. Rothman, R. R. Gamache, and A. Goldman, 2006, *J. Quant. Spectrosc. Radiat. Transfer* **98**(1), 130.

[66] Simmons, A. C., 1978, *Opt. Commun.* **25**(2), 211.

[67] Slanina, Z., F. Uhlík, S.-L. Lee, and S. Nagase, 2006, *J. Quant. Spectrosc. Radiat. Transfer* **97**(3), 415.

[68] Smith, K. M., I. Ptashnik, D. A. Newnham, and K. P. Shine, 2004, *J. Quant. Spectrosc. Radiat. Transfer* **83**(3–4), 735.

[69] Tanaka, T., M. Fukabori, T. Sugita, H. Nakajima, T. Yokota, T. Watanabe, and Y. Sasano, 2006, *J. Mol. Spectr.* **239**(1), 1.

[70] Toth, R. A., L. R. Brown, M. A. H. Smith, V. Malathy Devi, D. C. Benner, and M. Dulick, 2005, *J. Quant. Spectrosc. Radiat. Transfer* **101**(2), 339.

[71] Tubbs, R. N., J. A. Meisner, E. J. Bakker, and S. Albrecht, 2004, in *Astronomical Telescopes and Instrumentation*, edited by W. A. Traub (Int. Soc. Optical Engineering), volume 5491 of *Proc. SPIE*, pp. 588–599.

[72] Velsko, S. P., and D. Eimerl, 1986, *Appl. Opt.* **25**(8), 1344.

[73] Wagner, W., and A. Prüß, 2002, *J. Phys. Chem. Ref. Data* **31**(2), 387.

[74] Weber, L. A., 1970, *J. Res. Nat. Bur. Stand.* **74A**(1), 93.

[75] Yan, M., H. R. Sadeghpour, and A. Dalgarno, 1998, *Astrophys. J.* **496**(2), 1044, E: [76].

[76] Yan, M., H. R. Sadeghpour, and A. Dalgarno, 2001, *Astrophys. J.* **559**(2), 1194.

[77] Yang, Z., G. C. Toon, J. S. Margolis, and P. O. Wennberg, 2002, *Geophys. Res. Lett.* **29**(9), 53.

[78] Zhang, J., Z. H. Lu, and L. J. Wang, 2005, *Opt. Lett.* **30**(24), 3314.

[79] Zhenhui, W., and Z. Peichang, 2004, *J. Quant. Spectrosc. Radiat. Transfer* **83**(3–4), 423.